Electronic Supplementary Material (ESI) for Materials Advances.

Design and development of a new flowable and photocurable lactide and caprolactone-based polymer for bone repair and augmentation

Hamidi AS[a], Hadis MA[a], Williams RL[b], Grover LM[b], Palin WM[a*]

[a] *Dental and Biomaterials Science, School of Dentistry, College of Medical and Dental Science, Institute of Clinical Sciences, University of Birmingham, 5 Mill Pool Way, Edgbaston, Birmingham, B5 7EG, UK.*

[b] *Healthcare Technologies Institute (HTI), School of Chemical Engineering, University of Birmingham, Edgbaston, Birmingham, B15 2TT, UK*

Supplementary Data – 1B

1 Absolute irradiances and molar absorptivity

The absolute irradiance of AURA and EPSE Vario, represented by area integral under an irradiance curve, were measured using a miniature UV-Vis spectrometer (USB4000; Ocean Optics, USA), equipped with a 400 μm optical fiber that was coupled to an opal glass cosine corrector (CC3-UV, sensor diameter: 3.9 mm). Prior to any measurements, the spectrophotometer setup was calibrated with a deuterium (UV) and halogen (Visible-NIR) calibration light source (DH-2000-CAL; Ocean Optics, Florida, USA), as per NIST standards. Figure 1b displays emission spectra of AURA and ESPE Vario.

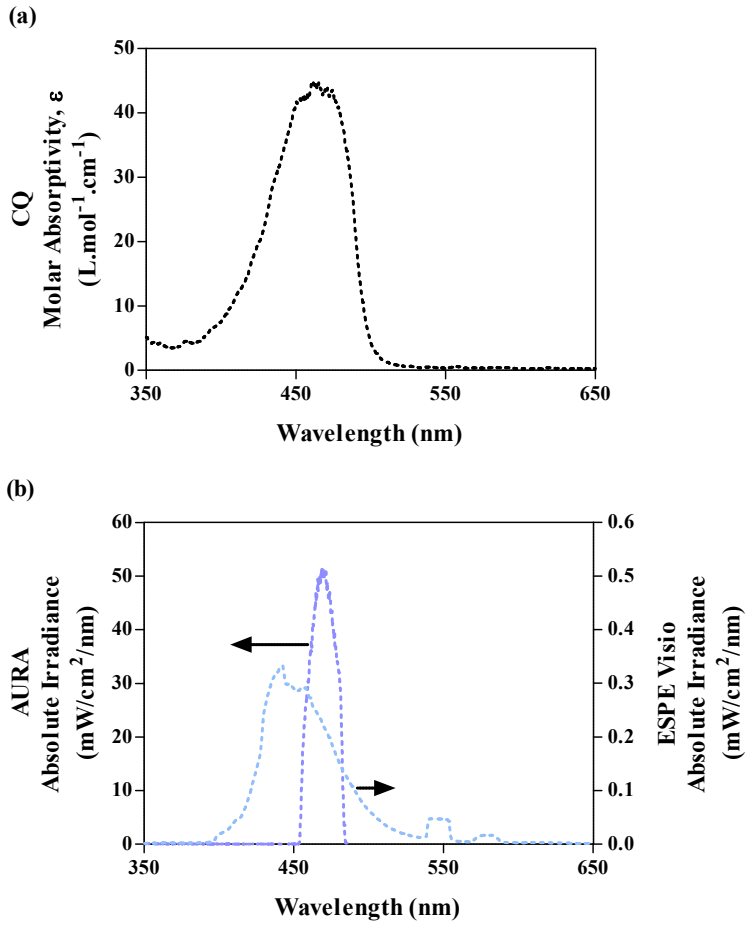

Figure 1: (a) Molar Absorptivity (Right axis) of CQ in pure methanol (1.11 x 10^{-4} mol/mL), measured using a miniature UV-Vis spectrophotometer (USB400). (b) Spectral irradiances of light curing units, used in present study.

2 *GPC* - $\bar{M}_n$ and $\bar{M}_w$ of Monomers

MW averages of monomers were determined using GPC, which involved molecular size separation based on hydrodynamic elution volume. However, since a constant flow rate of 1.0 mL/min was used, separation of molecules was measured in retention time (minutes) instead. Figure 2 and 3 illustrate chromatograms of both monomers. Elution peaks highlighted by green gridlines represent the distribution of monomer chain sizes as a function of retention time and RI. High MW chains (large coiled-up polymers) eluted first and marked the upper limit, while small polymer chains eluted last marking the lower limit.

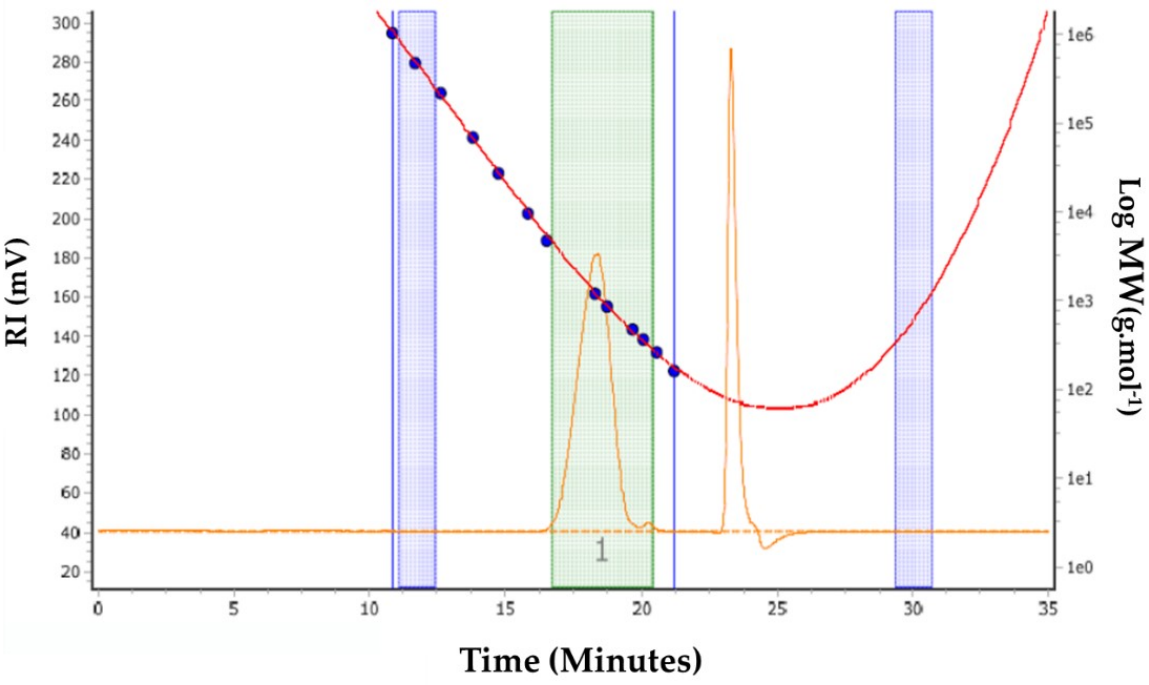

Figure 2: Chromatogram of PLLA-DM (SP-POL-116). Courtesy of SP (Montpelier, France).

Relative number ($\bar{M}_n$) and weight ($\bar{M}_w$), along with polydispersity index (PDI) was generated using the calibration curve. It is worth noting that the narrow peak at about 23 minutes corresponds to an additive, generally introduced to ensure more uniform flow and/or avoid non-size exclusion interactions with the column [99]. Variation in M_n, M_w and PDI among three PLLA-DM batches were ± 6.85, 6.60 and 3.63 %, respectively. Equally, variation among PCF-DM batches were ± 11.36, 18.60 and 7.23 %, respectively.

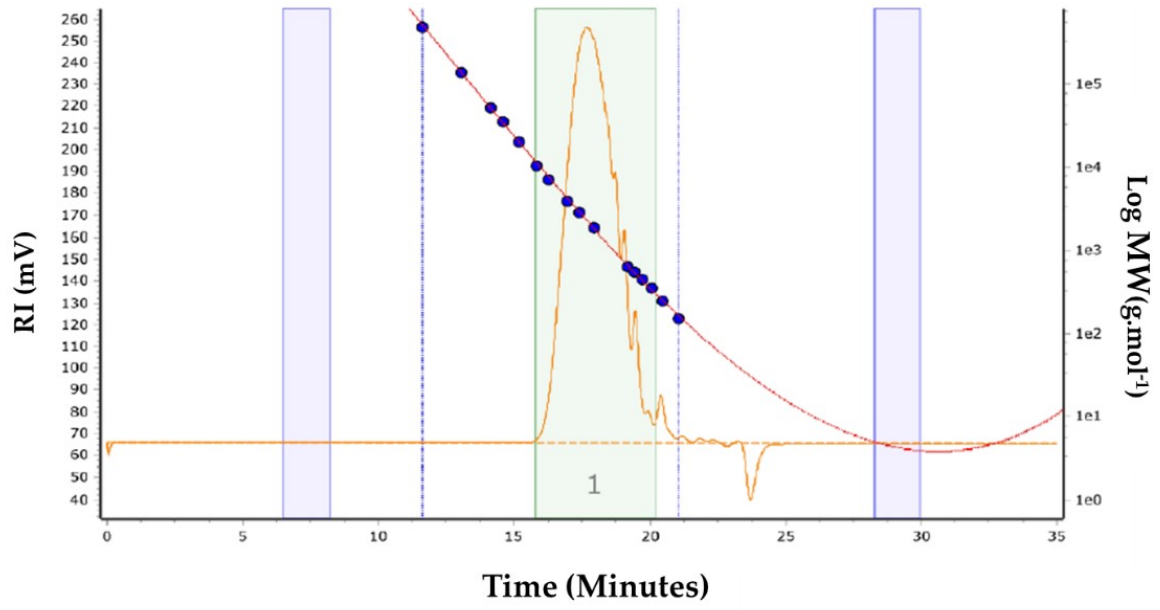

Figure 3: Chromatogram of PCF–DM (SP–POL–132). Courtesy of SP (Montpelier, France).

3 Apparent viscosity and flow behaviour

3.1 Methods

Apparent viscosities of unpolymerised neat monomers and their respective formulations were determined using Discovery Hybrid Rheometer HR1 (TA instruments, Brusselsesteenweg, Belgium). To measure viscosity as a function of strain, a shear rate sweep of 1 to 2000 s^{-1} was performed using a 20 mm cone-on-plate geometry with a cone angle of 2° and truncation height/gap (between the cone and a plate) of 53 µm. The geometry setup was calibrated for inertial, frictional, and rotational mapping prior to any measurements. Shear rate change and data acquisition were acquired algorithmically (Log_{10}) by dispensing 0.10 mL of monomer sample between the cone and a plate using a 1 mL syringe. Plate temperature was adjusted accordingly (25 / 37°C), with an initial 60 s 'temperature soaking time'. Viscosity measurements were conducted in triplicates per monomer / formulation and per temperature group. Data were analysed using TRIOS software (v5.0.0).

3.2 Results

Figure 4 depicts apparent viscosities of monomer formulations, as a function of shear rate (s^{-1}) at 25^{o}C (Figure 4a) and 37^{o}C (Figure 4b). Two-way ANOVA analysis revealed significant reduction ($P < 0.05$) in apparent viscosities as a function of shear rate (1/s) and operating (environmental) temperature.

At 25^{o}C, the effect of high-speed shearing was more apparent for formulations containing higher PLLA-DM content (F4 and F5). Fluid shear thinning (Flow Index, $n < 1$) was significant with greater reduction in apparent viscosities (Post hoc, Bonferroni, $P < 0.05$), when compared with F1–3 formulations which displayed relatively gradual shear thinning behaviours.

An increase in temperature (to 37^{o}C) led to significant decline ($P < 0.05$), with as much as 77 and 86 % reduction in apparent viscosities of F4 and F5 formulations when compared at 100 shear rate (s^{-1}) under 25^{o}C operating temperature, respectively. Equally, formulations with lower PLLA-DM content (F1–F3), apparent viscosities were reduced by 60 to 70 %, when compared at 100 shear rate (s^{-1}) under 25^{o}C ($P < 0.05$). It is worth noting that the influence of shear rate under 37^{o}C was less noticeable with non-significant ($P > 0.05$) reduction in apparent viscosities at various shear rate steps for each formulation.

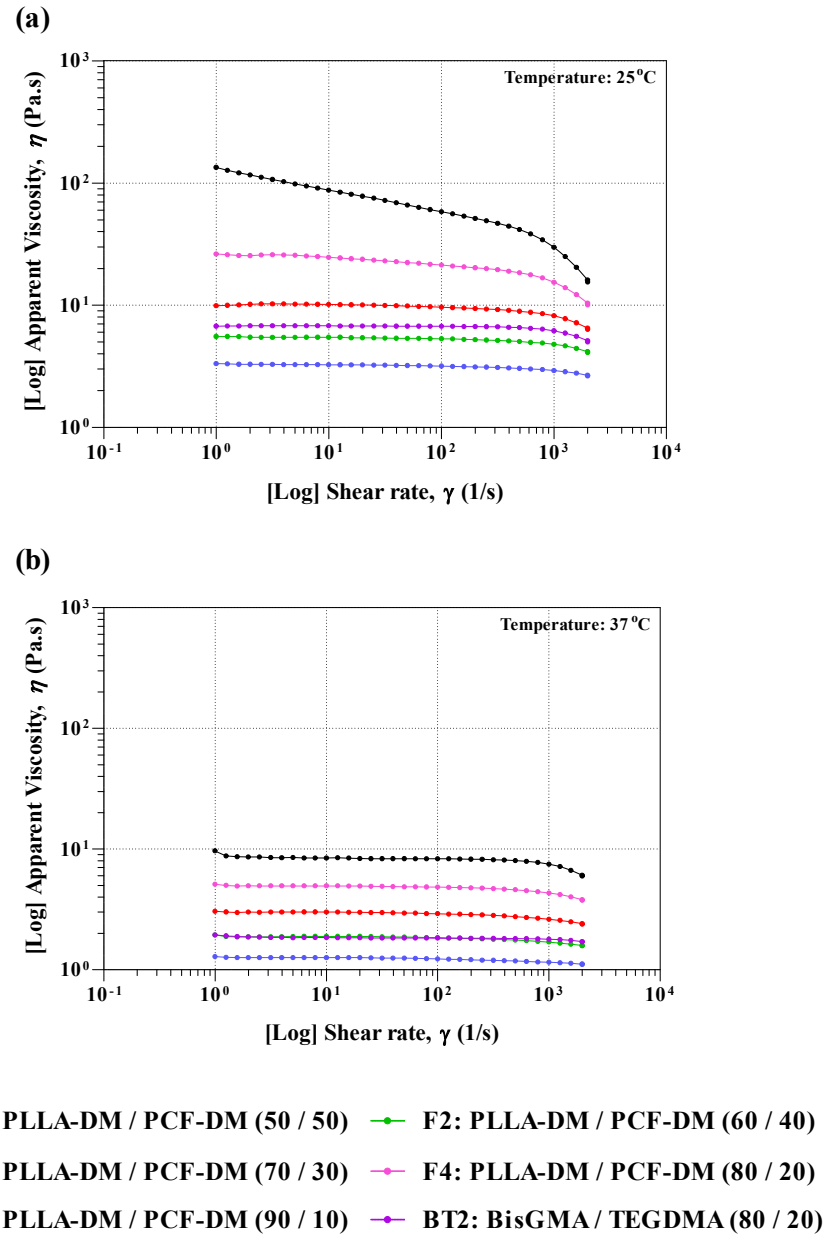

Figure 4: Apparent viscosities of unpolymerised formulations under a shear rate sweep of 1-2000 (s^{-1}) at 25 (a) and 37°C (b) operating temperatures with a temperature soaking time of 60 s.

3.3 Discussion

Generally, monomer formulations exhibited shear thinning behaviour which was more apparent for formulations containing higher PLLA-DM content. Propensity towards applied shear stresses might be attributed to higher intermolecular forces and entanglement of chains than PCF-DM. This may explain somewhat the 'sticky wax' nature of neat PLLA-DM as opposed

to the ‘oily’ texture observed for neat PCF-DM. The effect of temperature on apparent viscosities of formulations was more influential than shearing. Increased temperature may have led polymer chains to gain enough energy to overcome intermolecular interactions and disrupt entanglement from the bulk structure [100]. As a result, resistance to flow (viscosity) decreased and polymer networks began to flow more readily.

A significant reduction in the apparent viscosity of F5 at relatively low shear rates under 25^{o}C might be attributed to the ‘*Weissenburg effect*’, caused by normal stress forces generated during shear deformation. A phenomenon commonly occurs in paints and polymer solutions involving an elastic fluid mixed in a highly viscous solvent. PCF-DM chains may have experienced relatively larger elastic deformation and stretching than PLLA-DM under the same shear stresses away from the centre. In cone-on-plate geometry, this can create outward normal forces which in turn affect polymer contact with cone and the plate [100-102].

4 References

1. GrandViewResearch, *Orthopedic Implants Market Analysis, By Application (Spinal fusion, Long bone, Foot & Ankle, Craniomaxillofacial, Joint replacement, Dental), And Segment Forecasts To 2024*, in *Medical Devices*. 2016.
2. Hasan, A., et al., *Advances in osteobiologic materials for bone substitutes.* J Tissue Eng Regen Med, 2018. **12**(6): p. 1448-1468.
3. GrandViewResearch, *Bone Grafts And Substitutes Market Size, Share & Trends Analysis Report By Material Type (Allograft, Synthetic), By Application Type (Spinal Fusion, Craniomaxillofacial, Long Bone), By Region, And Segment Forecasts, 2019 - 2026*. 2019. p. 126.
4. Böker, K.O., et al., *Current State of Bone Adhesives-Necessities and Hurdles.* Materials (Basel, Switzerland), 2019. **12**(23): p. 3975.
5. Leggat, P.A., D.R. Smith, and U. Kedjarune, *Surgical applications of cyanoacrylate adhesives: a review of toxicity.* ANZ J Surg, 2007. **77**(4): p. 209-13.
6. Gheduzzi, S., J. Webb, and A. Miles, *Mechanical characteristics of three percutaneous vertebroplasty biomaterials.* Journal of materials science. Materials in medicine, 2006. **17**: p. 421-6.
7. Heraeus-Medical. *Osteopal Family*. 2020; Available from: https://www.heraeus.com/en/hme/products_solutions_heraeus_medical/spinal_augmentation/osteopal_vertebral_compression_fractures.html.
8. Heraeus-Medical. *Palacos Family*. 2020; Available from: https://www.heraeus.com/en/hme/products_solutions_heraeus_medical/arthrosis/palacos_bone_cements.html.
9. Heraeus-Medical. *Copal G+C - Bone cement with genamicin and clindamycin*. 2020 30 April 2020]; Available from: https://www.heraeus.com/en/hme/products_solutions_heraeus_medical/overview_products_indication/copal_gc_antibiotics.html.
10. Stryker. *SpinePlex bone cement*. 2020 30 April 2020]; Available from: https://www.stryker.com/us/en/interventional-spine/products/spineplex-cement.html.
11. McSweeney, A.L., et al., *Biocompatibility, bone healing, and safety evaluation in rabbits with an IlluminOss bone stabilization system.* Journal of orthopaedic research : official publication of the Orthopaedic Research Society, 2017. **35**(10): p. 2181-2190.
12. PRLOG. *Swiss Ozics Group Announces CE Mark for the CompO6 (TM) Bone Reinforcement Composite. Ozics Group*. 2011 30 April 2020]; Available from: https://www.prlog.org/11712867-swiss-ozics-group-announces-ce-mark-for-the-compo6-tm-bone-reinforcement-composite.html.
13. Stryker. *Costoss bone augmentation material*. 2020; Available from: https://www.stryker.com/us/en/interventional-spine/products/cortoss-bone-augmentation-material.html.
14. Juvonen, T., et al., *Biomechanical evaluation of bone screw fixation with a novel bone cement.* Biomedical engineering online, 2015. **14**: p. 74-74.
15. Gergely, R.C.R., et al., *Towards the optimization of the preparation procedures of PMMA bone cement.* Journal of Orthopaedic Research, 2016. **34**(6): p. 915-923.
16. Kurata, S., K. Morishita, T. Kawase, and K. Umemoto, *Cytotoxic effects of acrylic acid, methacrylic acid, their corresponding saturated carboxylic acids, HEMA, and hydroquinone on fibroblasts derived from human pulp.* Dent Mater J, 2012. **31**(2): p. 219-25.

17. Lai, P.L., L.H. Chen, W.J. Chen, and I.M. Chu, *Chemical and physical properties of bone cement for vertebroplasty.* Biomed J, 2013. **36**(4): p. 162-7.
18. Palussière, J., et al., *Clinical results of an open prospective study of a bis-GMA composite in percutaneous vertebral augmentation.* European Spine Journal, 2005. **14**(10): p. 982-991.
19. Teeguarden, J.G. and S. Hanson-Drury, *A systematic review of Bisphenol A "low dose" studies in the context of human exposure: a case for establishing standards for reporting "low-dose" effects of chemicals.* Food Chem Toxicol, 2013. **62**: p. 935-48.
20. Krifka, S., G. Spagnuolo, G. Schmalz, and H. Schweikl, *A review of adaptive mechanisms in cell responses towards oxidative stress caused by dental resin monomers.* Biomaterials, 2013. **34**(19): p. 4555-63.
21. Long, P.H., *Medical devices in orthopedic applications.* Toxicol Pathol, 2008. **36**(1): p. 85-91.
22. Ferreira, P., J.F.J. Coelho, J.F. Almeida, and M.H. Gil, *Photocrosslinkable Polymers for Biomedical Applications.* Biomedical Engineering - Frontiers and Challenges, 2011: p. 55-74.
23. van Bochove, B. and D.W. Grijpma, *Photo-crosslinked synthetic biodegradable polymer networks for biomedical applications.* Journal of Biomaterials Science, Polymer Edition, 2019. **30**(2): p. 77-106.
24. Fisher, J.P., D. Dean, and A.G. Mikos, *Photocrosslinking characteristics and mechanical properties of diethyl fumarate/poly(propylene fumarate) biomaterials.* Biomaterials, 2002. **23**(22): p. 4333-4343.
25. Timmer, M.D., C.G. Ambrose, and A.G. Mikos, *In vitro degradation of polymeric networks of poly(propylene fumarate) and the crosslinking macromer poly(propylene fumarate)-diacrylate.* Biomaterials, 2003. **24**(4): p. 571-7.
26. Jabbari, E., et al., *Synthesis, material properties, and biocompatibility of a novel self-cross-linkable poly(caprolactone fumarate) as an injectable tissue engineering scaffold.* Biomacromolecules, 2005. **6**(5): p. 2503-11.
27. Wang, S., et al., *Synthesis and characterizations of biodegradable and crosslinkable poly(ε-caprolactone fumarate), poly(ethylene glycol fumarate), and their amphiphilic copolymer.* Biomaterials, 2006. **27**(6): p. 832-841.
28. Lee, K.-W., S. Wang, M.J. Yaszemski, and L. Lu, *Physical properties and cellular responses to crosslinkable poly(propylene fumarate)/hydroxyapatite nanocomposites.* Biomaterials, 2008. **29**(19): p. 2839-2848.
29. Alge, D.L., et al., *Poly(propylene fumarate) reinforced dicalcium phosphate dihydrate cement composites for bone tissue engineering.* J Biomed Mater Res A, 2012. **100**(7): p. 1792-802.
30. Liu, X., et al., *Novel biodegradable poly(propylene fumarate)-co-poly(l-lactic acid) porous scaffolds fabricated by phase separation for tissue engineering applications.* RSC Advances, 2015. **5**(27): p. 21301-21309.
31. Wang, L., D.-G. Guo, H. Zhu, and L. Xie, *Light emitting diodes (LEDs) encapsulation of polymer composites based on poly(propylene fumarate) crosslinked with poly(propylene fumarate)-diacrylate.* RSC Advances, 2015. **5**(65): p. 52888-52895.
32. Hughes, A., H. Tai, A. Tochwin, and W. Wang, *Biodegradable and Biocompatible PDLLA-PEG1k-PDLLA Diacrylate Macromers: Synthesis, Characterisation and Preparation of Soluble Hyperbranched Polymers and Crosslinked Hydrogels.* Processes, 2017. **5**: p. 18.
33. Chocholata, P., V. Kulda, and V. Babuska, *Fabrication of Scaffolds for Bone-Tissue Regeneration.* Materials (Basel, Switzerland), 2019. **12**(4): p. 568.

34. Gunatillake, P.A. and R. Adhikari, *Biodegradable synthetic polymers for tissue engineering.* Eur Cell Mater, 2003. **5**: p. 1-16; discussion 16.
35. Hsu, S.-h., K.-C. Hung, and C.-W. Chen, *Biodegradable polymer scaffolds.* Journal of Materials Chemistry B, 2016. **4**(47): p. 7493-7505.
36. Masutani, K. and Y. Kimura, *Chapter 1 PLA Synthesis. From the Monomer to the Polymer*, in *Poly(lactic acid) Science and Technology: Processing, Properties, Additives and Applications*. 2015, The Royal Society of Chemistry. p. 1-36.
37. Maharana, T., B. Mohanty, and Y.S. Negi, *Melt–solid polycondensation of lactic acid and its biodegradability.* Progress in Polymer Science, 2009. **34**(1): p. 99-124.
38. Wei, S., et al., *Biodegradable materials for bone defect repair.* Military Medical Research, 2020. **7**(1): p. 54.
39. Zhang, C., *Biodegradable Polyesters: Synthesis, Properties, Applications. First Edition*, ed. S. Fakirov. 2015: Wiley-VCH Verlag GmbH & Co.KGaA.
40. Broz, M.E., D.L. VanderHart, and N.R. Washburn, *Structure and mechanical properties of poly(d,l-lactic acid)/poly(ε-caprolactone) blends.* Biomaterials, 2003. **24**(23): p. 4181-4190.
41. Laycock, B., et al., *Lifetime prediction of biodegradable polymers.* Progress in Polymer Science, 2017. **71**: p. 144-189.
42. Shi, R., et al., *Structure, physical properties, biocompatibility and in vitro/vivo degradation behavior of anti-infective polycaprolactone-based electrospun membranes for guided tissue/bone regeneration.* Polymer Degradation and Stability, 2014. **109**: p. 293-306.
43. Ho, S.-M. and A.M. Young, *Synthesis, polymerisation and degradation of poly(lactide-co-propylene glycol) dimethacrylate adhesives.* European Polymer Journal, 2006. **42**(8): p. 1775-1785.
44. Young, A.M. and S.M. Ho, *Drug release from injectable biodegradable polymeric adhesives for bone repair.* J Control Release, 2008. **127**(2): p. 162-72.
45. Young, A.M., et al., *Chemical characterization of a degradable polymeric bone adhesive containing hydrolysable fillers and interpretation of anomalous mechanical properties.* Acta Biomater, 2009. **5**(6): p. 2072-83.
46. E.A. Abou Neel, G.P., J.C. Knowles, V. Salih, A.M. Young, *Chemical, modulus and cell attachment studies of reactive calcium phosphate filler-containing fast photo-curing, surface-degrading, polymeric bone adhesives.* Acta Biomaterialia, 2010. **6**: p. 2695-2703.
47. Zhao, X., et al., *Reactive calcium-phosphate-containing poly(ester-co-ether) methacrylate bone adhesives: Chemical, mechanical and biological considerations.* Acta Biomaterialia, 2010. **6**(3): p. 845-855.
48. Gellynck, K., et al., *Cell attachment and response to photocured, degradable bone adhesives containing tricalcium phosphate and purmorphamine.* Acta Biomater, 2011. **7**(6): p. 2672-7.
49. Abou Neel, E.A., V. Salih, P.A. Revell, and A.M. Young, *Viscoelastic and biological performance of low-modulus, reactive calcium phosphate-filled, degradable, polymeric bone adhesives.* Acta Biomaterialia, 2012. **8**(1): p. 313-320.
50. Abou Neel, E.A., V. Salih, P.A. Revell, and A.M. Young, *Brushite and Self-Healing Flexible Polymer-Modified Brushite Bone Adhesives for Fibular Osteotomy Repair.* Advanced Engineering Materials, 2014. **16**(2): p. 218-230.
51. Runge, M.B., et al., *Reformulating polycaprolactone fumarate to eliminate toxic diethylene glycol: effects of polymeric branching and autoclave sterilization on material properties.* Acta Biomater, 2012. **8**(1): p. 133-43.

52. Lipik, V.T., et al., *Thermoplastic biodegradable elastomers based on ε-caprolactone and l-lactide block co-polymers: A new synthetic approach.* Acta Biomaterialia, 2010. **6**(11): p. 4261-4270.
53. Shinno, K., et al., *Solid-State Postpolymerization of l-Lactide Promoted by Crystallization of Product Polymer: An Effective Method for Reduction of Remaining Monomer.* Macromolecules, 1997. **30**(21): p. 6438-6444.
54. Wang, Z., et al., *Preparation and rapid degradation of nontoxic biodegradable polyurethanes based on poly(lactic acid)-poly(ethylene glycol)-poly(lactic acid) and l-lysine diisocyanate.* Polymer Chemistry, 2011. **2**(3): p. 601-607.
55. Kaihara, S., S. Matsumura, A.G. Mikos, and J.P. Fisher, *Synthesis of poly(L-lactide) and polyglycolide by ring-opening polymerization.* Nat Protoc, 2007. **2**(11): p. 2767-71.
56. He, S., et al., *Synthesis of biodegradable poly(propylene fumarate) networks with poly(propylene fumarate)–diacrylate macromers as crosslinking agents and characterization of their degradation products.* Polymer, 2001. **42**(3): p. 1251-1260.
57. Sigma-Aldrich. *Polymer Analysis by NMR*. 2006; Available from: https://www.sigmaaldrich.com/technical-documents/articles/material-matters/polymer-analysis-by.html.
58. Bacher, A. *Infrared Spectroscopy*. 2002 30 April 2020]; Available from: http://www.chem.ucla.edu/~bacher/spectrocopy/IR1.html.
59. Albuquerque, P.P.A.C., et al., *Color stability, conversion, water sorption and solubility of dental composites formulated with different photoinitiator systems.* Journal of Dentistry, 2013. **41**: p. e67-e72.
60. Hansen U, Z.P., Simpson R, Currey J D, Hynd D. , *The Effect of Strain Rate on the Mechanical Properties of Human Cortical Bone.* Journal of Biomechanical Engineering, 2008. **130**: p. 110-118.
61. Zange R, L.Y., Kissel T, *Biocompatibility testing of ABA triblock copolymers consisting of poly(L-lactic-co-glycolic acid) A blocks attached to a central poly(ethylene oxide) B block under in vitro conditions using different L929 mouse fibroblasts cell culture models.* Journal of Controlled Release, 1998. **56**: p. 249-258.
62. Sittampalam, G.S., L. Eli, Company, and S. National Center for Advancing Translational, *Assay guidance manual.* 2004: p. 263-267.
63. Thermofisher. *Protocol for Passaging Adherent Cells*. 2016 [cited 2016; Available from: https://www.thermofisher.com/uk/en/home/references/gibco-cell-culture-basics/cell-culture-protocols/subculturing-adherent-cells.html.
64. Hausser, H.-J. and R.E. Brenner, *Phenotypic instability of Saos-2 cells in long-term culture.* Biochemical and Biophysical Research Communications, 2005. **333**(1): p. 216-222.
65. Invitrogen_Corporation. *alamarBlue Assay manual (PI-DAL1025/1100Rev 1.0)*. 2002; Available from: http://tools.invitrogen.com/content/sfs/manuals/PIDAL1025-1100_TI%20alamarBlue%20Rev%201.1.pdf.
66. Longo, G., et al., *Improving Osteoblast Response In Vitro by a Nanostructured Thin Film with Titanium Carbide and Titanium Oxides Clustered around Graphitic Carbon.* PloS one, 2016. **11**: p. e0152566.
67. Zeng, J.-B., et al., *A novel biodegradable multiblock poly(ester urethane) containing poly(l-lactic acid) and poly(butylene succinate) blocks.* Polymer, 2009. **50**(5): p. 1178-1186.
68. Karikari, A.S., W.F. Edwards, J.B. Mecham, and T.E. Long, *Influence of Peripheral Hydrogen Bonding on the Mechanical Properties of Photo-Cross-Linked Star-Shaped Poly(d,l-lactide) Networks.* Biomacromolecules, 2005. **6**(5): p. 2866-2874.

69. Pautke, C., et al., *Characterization of osteosarcoma cell lines MG-63, Saos-2 and U-2 OS in comparison to human osteoblasts.* Anticancer Res, 2004. **24**(6): p. 3743-8.
70. Ayobian-Markazi, N., T. Fourootan, and M.J. Kharazifar, *Comparison of cell viability and morphology of a human osteoblast-like cell line (SaOS-2) seeded on various bone substitute materials: An in vitro study.* Dental research journal, 2012. **9**(1): p. 86-92.
71. Becker, H. and H. Vogel, *The Role of Hydroquinone Monomethyl Ether in the Stabilization of Acrylic Acid.* Chemical Engineering & Technology, 2006. **29**(10): p. 1227-1231.
72. Jakubiak, J., et al., *Camphorquinone–amines photoinitating systems for the initiation of free radical polymerization*. Vol. 44. 2003. 5219-5226.
73. Kwon, T.Y., et al., *Cure mechanisms in materials for use in esthetic dentistry.* J Investig Clin Dent, 2012. **3**(1): p. 3-16.
74. Hamidi AS, H.M., WM Palin, *Alternative co-Initiators for photocurable dental resins: Polymerisation, quantum yield of conversion and cytotoxicity.* Dent Materials, 2022. **38**(8): p. 1330-1343.
75. Davidenko, N., O. García, and R. Sastre, *Photopolymerization kinetics of dimethacrylate-based light-cured dental resins.* Journal of Applied Polymer Science, 2005. **97**(3): p. 1016-1023.
76. Leprince, J.G., et al., *Progress in dimethacrylate-based dental composite technology and curing efficiency.* Dental Materials, 2013. **29**(2): p. 139-156.
77. Ballo, A.M., et al., *Osseointegration of fiber-reinforced composite implants: Histological and ultrastructural observations.* Dental Materials, 2014. **30**(12): p. e384-e395.
78. Lin, N.J. and S. Lin-Gibson, *Osteoblast response to dimethacrylate composites varying in composition, conversion and roughness using a combinatorial approach.* Biomaterials, 2009. **30**(27): p. 4480-4487.
79. Wang, L., J. Qiu, and E. Sakai, *Microstructures and mechanical properties of polylactic acid prepared by a cold rolling process.* Journal of Materials Processing Technology, 2016. **232**: p. 184-194.
80. Zhao, H. and G. Zhao, *Mechanical and thermal properties of conventional and microcellular injection molded poly (lactic acid)/poly (ε-caprolactone) blends.* Journal of the Mechanical Behavior of Biomedical Materials, 2016. **53**: p. 59-67.
81. Douglas, P., et al., *Thermo-mechanical properties of poly ε-caprolactone/poly l-lactic acid blends: Addition of nalidixic acid and polyethylene glycol additives.* Journal of the Mechanical Behavior of Biomedical Materials, 2015. **45**: p. 154-165.
82. Malinowski, R., *Mechanical properties of PLA/PCL blends crosslinked by electron beam and TAIC additive.* Chemical Physics Letters, 2016. **662**: p. 91-96.
83. Stockwell, R., *The Mechanical Properties of Biological Materials.* Journal of Anatomy, 1981. **133(Pt 1)**: p. 99-100.
84. Ekaterina N, P.-Y.C., Elham H, Li Jun, Vlado A L, Iwona J, Joanna M., *Recent advances on the measurement and calculation of the elastic moduli of cortical and trabecular bone: A review.* Theoretical and Applied Mechanics 2011, 2011. **38**(3): p. 209-297.
85. Hart, N.H., et al., *Mechanical basis of bone strength: influence of bone material, bone structure and muscle action.* Journal of musculoskeletal & neuronal interactions, 2017. **17**(3): p. 114-139.
86. Spector, J.M., BJ; Greenwald, JA; Saadeh, PB; Steinbrech, DS; Bouletreau, PJ; Smith, LP; Longaker, MT., *Osteoblast expression of vascular endothelial growth factor is modulated by the extracellular microenvironment.* American Journal of Physiology. Cell Physiology, 2001. **280**(C72).

87. Hardin, C.C. and J.A. Knopp, *23.1 Pathway*, in *Biochemistry - Essential Concepts*. Oxford University Press.
88. Kumari, A., *Chapter 1 - Glycolysis*, in *Sweet Biochemistry*, A. Kumari, Editor. 2018, Academic Press. p. 1-5.
89. DANIELLE S.W. BENOIT, A.R.D., KRISTI S. ANSETH1, *Manipulations in Hydrogel Degradation Behavior Enhance Osteoblast Function and Mineralized Tissue Formation.* TISSUE ENGINEERING, 2006. **12**(6): p. 1663-73.
90. Malikmammadov, E., et al., *PCL and PCL-based materials in biomedical applications.* Journal of Biomaterials Science, Polymer Edition, 2018. **29**(7-9): p. 863-893.
91. Caroline Alberici Martins, G.L., Werner Geurtsen, Joachim Volk, *Intracellular glutathione: A main factor in TEGDMA-induced cytotoxicity?* Dental Materials, 2012. **28**: p. 442-448.
92. Walters, N.J., et al., *Poly(propylene glycol) and urethane dimethacrylates improve conversion of dental composites and reveal complexity of cytocompatibility testing.* Dent Mater, 2016. **32**(2): p. 264-77.
93. H. Schweikla, A.H., K.-A. Hiller, G. Spagnuolo, C. Bolaya, G. Brockhoff, G. Schmalz, *Inhibition of TEGDMA and HEMA-induced genotoxicity and cell cycle arrest by N-acetylcysteine.* Dental Materials, 2007. **23**: p. 688-695.
94. G Spagnuolo, K.G., G Schmalz, C Cosentino, S Rengo, H Schweikl., *Inhibition of phosphatidylinositol 3-kinase amplifies TEGDMA-induced apoptosis in primary human pulp cells.* Journal of Dental Research, 2004. **83**: p. 703-7.
95. Helmut Schweikl, G.S., Kirsten Rackebrandt, *The mutagenic activity of unpolymerized resin monomers in Salmonella typhimurium and V79 cells.* Mutation Research, 1998. **415**: p. 119–130.
96. Abdal-hay, A., N.T. Raveendran, B. Fournier, and S. Ivanovski, *Fabrication of biocompatible and bioabsorbable polycaprolactone/ magnesium hydroxide 3D printed scaffolds: Degradation and in vitro osteoblasts interactions.* Composites Part B: Engineering, 2020. **197**: p. 108158.
97. Yin, H.-M., et al., *Nanotopographical polymeric surface with mussel-inspired decoration to enhance osteoblast differentiation.* Applied Surface Science, 2019. **481**: p. 987-993.
98. El-Amin, S.F., et al., *Extracellular matrix production by human osteoblasts cultured on biodegradable polymers applicable for tissue engineering.* Biomaterials, 2003. **24**(7): p. 1213-1221.
99. AgilentTechnologies, *An Introduction to Gel Permeation Chromatography and Size Exclusion Chromatography*. 2014.
100. Malkin, A.Y. and A. Isayev, *3.3.4.2 Viscosity of Polymer Solutions*, in *Rheology - Concept, Methods, and Applications (3rd Edition)*. 2017, ChemTec Publishing.
101. Clavier, R., *21.1 Viscosity*, in *Characterization and Analysis of Polymers*. 2008, John Wiley & Sons.
102. Malkin, A.Y., *4.1.1 Non-Newtonian Viscosity*, in *Rheology Fundamentals*. 1994, ChemTec Publishing.